A Molecular Mechanism for Electrical Tuning of Cochlear Hair Cells

Krishnan Ramanathan, Timothy H. Michael, Guo-Jian Jiang, Hakim Hiel, Paul A. Fuchs*

Cochlear frequency selectivity in lower vertebrates arises in part from electrical tuning intrinsic to the sensory hair cells. The resonant frequency is determined largely by the gating kinetics of calcium-activated potassium (BK) channels encoded by the *slo* gene. Alternative splicing of *slo* from chick cochlea generated kinetically distinct BK channels. Combination with accessory β subunits slowed the gating kinetics of α splice variants but preserved relative differences between them. In situ hybridization showed that the β subunit is preferentially expressed by low-frequency (apical) hair cells in the avian cochlea. Interaction of β with α splice variants could provide the kinetic range needed for electrical tuning of cochlear hair cells.

Acoustic analysis begins with the discrimination of individual frequency components within the cochlea. The sensory hair cells contribute to frequency selectivity through combinations of electrical and mechanical feedback whose relative importance differs among vertebrate species. For the low-frequency hearing of the turtle, electrical tuning of hair cells provides most of the filtering (*1*). This mechanism depends on the interplay between voltage-gated calcium channels and large-conductance calcium-activated potassium (BK) channels (*2, 3*). A 30-fold variation in BK channel kinetics determines the tuning frequency between 50 and 600 Hz (*4*). BK channels are encoded by the *slo* gene in chick hair cells (*5*), where they also support electrical tuning (*6*). It has been proposed that alternative splicing of the *slo* gene could provide the functional heterogeneity of hair cell BK channels, and numerous alternative exons of *slo* have been cloned from chick and turtle cochleas (*5, 7–9*). However, previous expression of several splice variants revealed little or no difference in steady-state or kinetic parameters (*8, 10*). We have since identified an alternative 183–base pair (bp) exon (AF076268) in chick hair cells [at splice site 2, *hslo* numbering (*11*)] that is identical to an exon cloned from the turtle cochlea (*9*) and is homologous to the Strex-2 exon from rat adrenal chromaffin cells (*12*). When this 61–amino acid exon was spliced into a full-length chick *slo* cDNA (*cSlo1*-U23821) (*13*), the encoded channels were kinetically distinct from the exonless form and were more calcium-sensitive. Furthermore, coexpression of these variant *slo* channels with accessory β subunits exaggerated their kinetic differences but diminished differences in calcium affinity.

Channels were studied by transient transfection of HEK 293 cells (*14*). α_{61} (the exon-added α variant) and α_0 (*cSlo1*) (*5*) were examined by voltage-clamp analysis of excised inside-out patches exposed to different concentrations of calcium (*15*). Currents flowing across patches expressing either α_0 or α_{61} in 5 μM calcium are overlaid for comparison in Fig. 1A. Tail current deactivation rates were consistently slower for α_{61}. The average deactivation time constants for a range of voltages in 5 μM calcium are shown for these two splice variants in Fig. 1B. On average, α_{61} decayed 2.5 times more slowly than did α_0 (similar results were obtained in Ca^{2+} concentrations ranging from 1 to 20 μM).

The voltage dependence of the channel was determined by measurement of the steady-state current amplitude as a function of the command voltage (Fig. 1C). When corrected for driving force, these values provided normalized conductance as a function of voltage and were fit with Boltzmann relations (*16*). The half-activation voltage ($V_{1/2}$) plotted as a function of calcium concentration illustrates the interdependence of calcium and

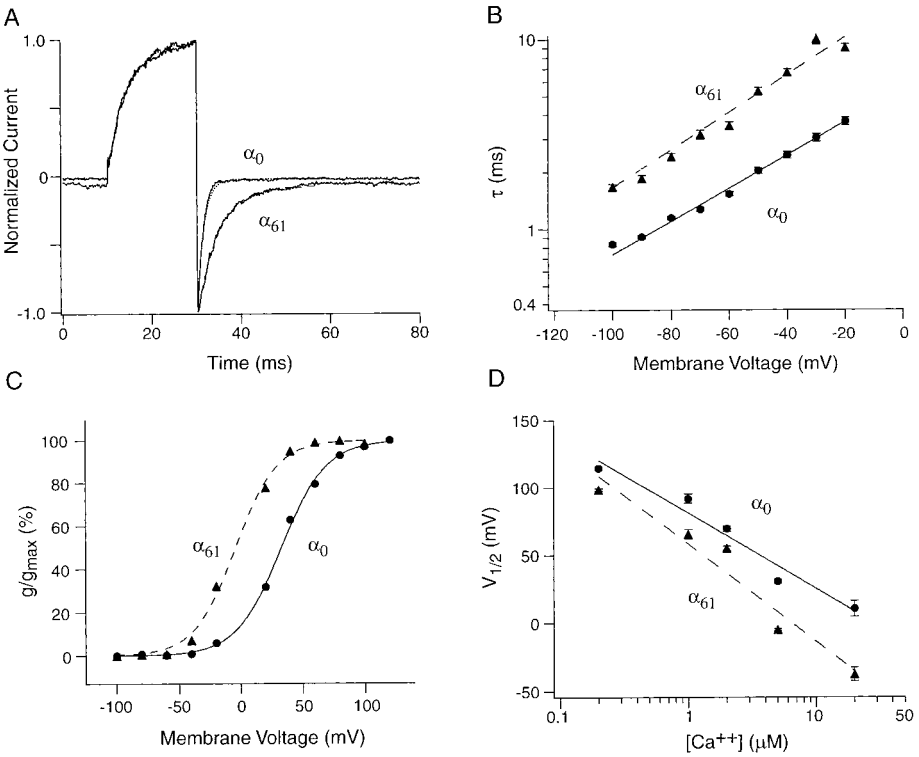

Fig. 1. α_0 and α_{61} differ in both kinetics and calcium sensitivity. (**A**) Normalized current traces from IOPs exposed to 5 μM Ca^{2+} and depolarized to 80 mV (*14*). Single exponentials were fit to tail currents at a −60-mV repolarization voltage to determine deactivation time constants (α_0: τ = 1.5 ms; α_{61}: τ = 4.8 ms). (**B**) Average deactivation time constants (τ) of IOPs (5 μM Ca^{2+}) plotted versus membrane voltage. (**C**) IOPs were exposed to 5 μM Ca^{2+}, and g/g_{max} was evaluated from steady-state conditions to generate a conductance-voltage plot. A Boltzmann fit yielded the following $V_{1/2}$ values: α_0, $V_{1/2}$ = 32.5 mV; α_{61}, $V_{1/2}$ = −4.4 mV (*16*). (**D**) Average $V_{1/2}$ data from patches exposed to Ca^{2+} concentrations ranging from 0.2 to 20 μM. The data were fit with straight lines (*21*) using a least-squares method that produced *R* values of 0.97 and 0.95 for α_0 and α_{61}, respectively.

K. Ramanathan, Center for Hearing Sciences, Department of Biomedical Engineering, Johns Hopkins University School of Medicine, Baltimore, MD 21205, USA. T. H. Michael, G.-J. Jiang, H. Hiel, Center for Hearing Sciences, Department of Otolaryngology–Head and Neck Surgery (HNS), Johns Hopkins University School of Medicine, Baltimore, MD 21205, USA. P. A. Fuchs, Center for Hearing Sciences, Departments of Otolaryngology–HNS and Biomedical Engineering, Johns Hopkins University School of Medicine, Baltimore, MD 21205, USA.

*To whom correspondence should be addressed. E-mail: pfuchs@bme.jhu.edu

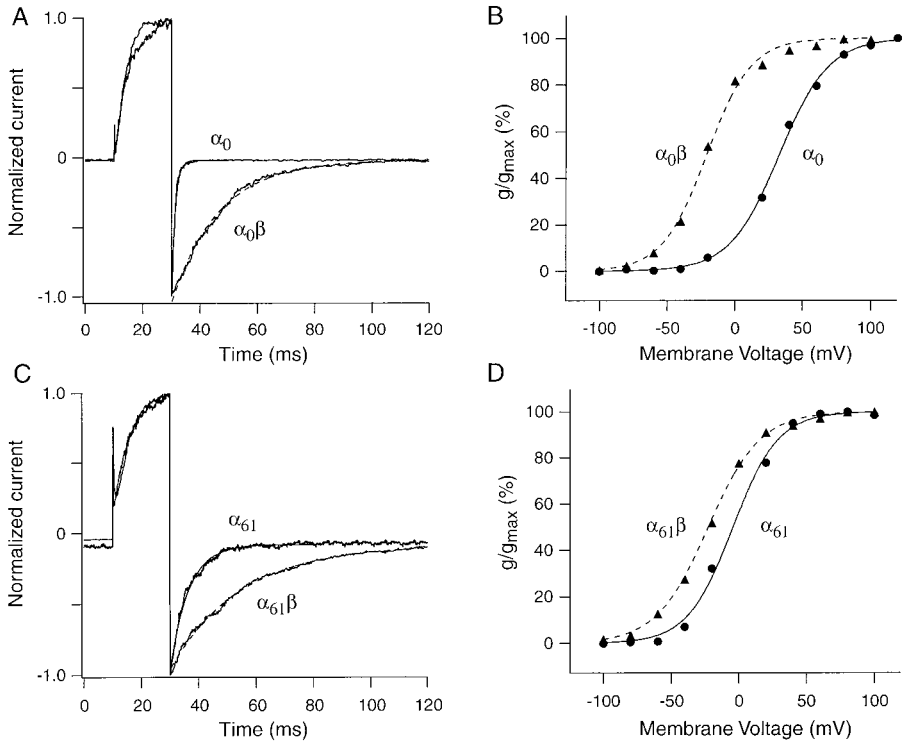

Fig. 2. Addition of β subunits shifts $V_{1/2}$ to more negative voltages and slows tail currents. (**A** and **C**) Tail currents at −100 mV in IOPs containing β with either α_0 or α_{61} (*14*). Coexpression of *slo*-β with α_0 (A) or α_{61} (C) results in a greater than 10-fold slowing of the deactivation rate. (**B** and **D**) g/g_{max} was evaluated from instantaneous tail currents and plotted against the activation voltage. Addition of the β subunit shifts the $V_{1/2}$ of both splice variants to more negative voltages ($V_{1/2}$ = 32.5 and −4.4 mV for α_0 and α_{61}; $V_{1/2}$ = −20.9 and −22.7 mV with β subunits added to α_0 and α_{61}, respectively) (*16*). The intracellular calcium concentration was 5 μM for these experiments.

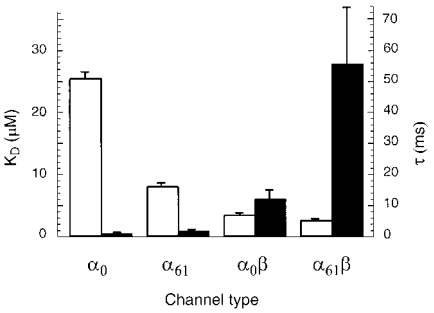

Fig. 3. The addition of β subunits to the two splice variants (α_0 and α_{61}) generates four kinetically distinct channels. Open bars are the dissociation constants (K_D) for Ca^{2+} binding at 0 mV. K_Ds were calculated from linear fits to $V_{1/2}$ versus log[Ca^{2+}] (*21*), shown in Fig. 1D. The time constant (τ, solid bars) of the decay of tail currents was measured in 5 μM Ca^{2+} at −100 mV. α_0 has the lowest affinity for Ca^{2+} and the fastest deactivation rate, whereas $\alpha_{61}\beta$ has the highest affinity for Ca^{2+} and the slowest deactivation rate.

voltage in *cSlo* channel gating. As calcium concentration rose, the channels activated at more negative membrane potentials. The resulting $V_{1/2}$ versus calcium plot for α_0 and α_{61} (Fig. 1D) shows that addition of the 61–amino acid exon caused a negative shift, equivalent to an increase in the channel's calcium sensitivity. These steady-state effects along with the slowing of deactivation rate were similar to those reported for the Strex-2 *slo* variant in adrenal chromaffin cells (*12*).

β subunits combine with and alter the calcium affinity and gating kinetics of mammalian *slo*-α channels (*17*), raising the question of whether avian hair cell *slo* behaves similarly. A presumptive quail *slo*-β (*18*) (U67865) was obtained and was coexpressed by mixture with *cSlo*-α cDNA before the transfection of HEK 293 cells (*19*). Combination of α_0 with β resulted in BK channels that had prolonged deactivation kinetics (Fig. 2A) (*20*). Decay time constants were more than 10 times larger with β addition. Combination with β also affected the steady-state gating parameters. The $V_{1/2}$ of $\alpha_0\beta$ in 5 μM calcium was more than 50 mV negative to that of α_0 alone (Fig. 2B). Similar effects were seen when *slo*-β was combined with α_{61}. Again, tail decay times were prolonged (Fig. 2C), and half activation occurred at more negative membrane potentials (Fig. 2D). These effects were observed at calcium concentrations from 1 to 20 μM.

The effects of β coexpression on these α splice variants are summarized in Fig. 3. Coexpression with β subunits greatly prolonged the deactivation time of both *cSlo*-α splice variants but preserved and even exaggerated kinetic differences between the variants. $\alpha_{61}\beta$ was five times slower than $\alpha_0\beta$, compared to the 2.5-fold kinetic difference between α subunits alone. It appears that β coexpression acts to amplify intrinsic kinetic differences between the α subunits, providing more than a 50-fold range in deactivation kinetics between α_0 and $\alpha_{61}\beta$. A still greater range of kinetic variability may be provided by other splice variants that have been described but remain to be characterized (*7–9*). For instance, it is expected that faster α forms will be required to match the fastest BK channels observed in turtle hair cells (*4*).

In addition, it should be noted that the $\alpha_{61}\beta$ combination had even greater calcium sensitivity and slower kinetics than are found in turtle hair cell BK channels. This raises the possibility that the saturation of α_{61} with β produced channels that might not be found naturally in hair cells. Further insight into β modification of *slo* channels is derived from consideration of its effects on steady-state parameters. Combination of α subunits with *slo*-β decreased the K_D (the calcium concentration needed to open half the channels at 0 mV) (Fig. 3) (*21*). When channel gating depends on both voltage and calcium, an increase in the calcium affinity of the channel's open state, relative to that of the closed state, could provide the slower deactivation and left-shifted voltage sensitivity seen with β coexpression.

Coexpression with β subunits exaggerated the kinetic differences among BK channels but minimized variations in calcium binding. The net effect was to give expressed channels the appearance of native BK channels whose kinetics, but not calcium affinity, vary with hair cell tuning (*4*). Additional support for the role of *slo*-β in hair cells was obtained with the use of reverse transcriptase polymerase chain reaction (RT-PCR) to amplify it from the quail cochlea (*22*). The expression pattern of *slo*-β in hair cells was examined with in situ hybridization (*23*), which revealed that *slo*-β mRNA was found particularly in apical (low-frequency) hair cells of the basilar papilla (Fig. 4). This is consistent with the hypothesis that β subunits combine with *slo*-α to produce low-frequency tuning (*24*). A further prediction is that some α splice variants, such as α_{61}, would experience lesser modulation by β if their expression were restricted to basal regions of the cochlea.

The present results show that β coexpression extends the kinetic range of *cSlo*-α splice variants whose intrinsic gating differs only modestly. Thus the combination of alternative splicing and β modulation may provide a molecular basis for the functional heterogeneity of BK channels that supports electrical tuning. Only two *slo*-α splice variants

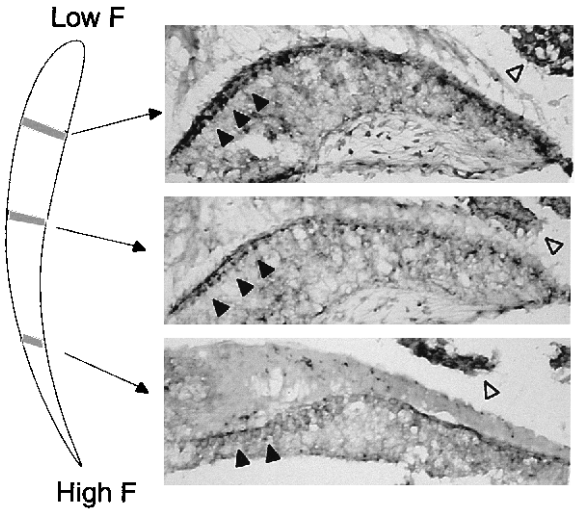

Fig. 4. *Slo*-β mRNA is expressed in quail hair cells. In situ hybridization was performed on cochlear cross sections (*23*). Solid arrowheads point to the rows of hair cells in the basilar papilla. The tonotopic positions of the sections are shown on the schematic cochlear duct [low frequency (F), apical end on top] at left. The tonotopic axis of the chick extends from 100 to 5000 Hz. Hair cell *slo*-β decreases from lowest to highest frequency regions. Label intensity in the tegmentum vasculosum (open arrowheads) did not vary systematically.

were studied here, and other alternate exons (*7–9*) may provide still further variation. Also, additional β subunits, as yet unknown, could provide still other forms of modulation to hair cell channels. The challenge remains to match particular channel proteins to the functional properties of an identified hair cell. Finally, the impressive conservation of channel function among the hair cells of amphibia, reptiles, and birds raises expectations that related molecular mechanisms will be found in the mammalian cochlea, where developmental changes in hair cell excitability (*25*) parallel the embryonic acquisition of BK channels in chick cochlear hair cells (*26*).

References and Notes

1. A. C. Crawford and R. Fettiplace, *J. Physiol.* **312**, 377 (1981).
2. J. J. Art and R. Fettiplace, *ibid.* **385**, 207 (1987).
3. J. Hudspeth and R. S. Lewis, *ibid.* **400**, 237 (1988).
4. J. J. Art, Y. C. Wu, R. Fettiplace, *J. Gen. Physiol.* **105**, 49 (1995).
5. G.-J. Jiang *et al.*, *Proc. R. Soc. London Ser. B.* **264**, 731 (1997).
6. P. A. Fuchs and M. G. Evans, *J. Comp. Physiol. A* **164**, 151 (1988); P. A. Fuchs, T. Nagai, M. G. Evans, *J. Neurosci.* **8**, 2460 (1988).
7. D. S. Navaratnam, T. J. Bell, T. D. Tu, E. L. Cohen, J. C. Oberholtzer, *Neuron* **19**, 1077 (1997).
8. K. P. Rosenblatt, Z. Sun, S. Heller, A. J. Hudspeth, *ibid.*, p. 1061.
9. E. M. C. Jones, C. Laus, R. Fettiplace, *Proc. R. Soc. London Ser. B.* **265**, 685 (1998).
10. T. Michael *et al.*, *Biophys. J.* **72**, A352 (1997).
11. J. Tseng-Crank *et al.*, *Neuron* **13**, 1315 (1994).
12. J. Xie and D. P. McCobb, *Science* **280**, 443 (1998).
13. *cSlo1* was cloned from a chick cochlear cDNA library (*5*). PCR of the cochlear cDNA library and RT-PCR of cochlear tissue identified the 61–amino acid insert. A chimeric construct incorporating the 61–amino acid insert was made by restriction digest and ligation of the PCR product with *cSlo1* and was packaged into pcDNA3.1 vector (Invitrogen, San Diego, CA) for transfection into mammalian cells.
14. HEK293 cells were transiently transfected by calcium phosphate precipitation. Inside-out patches (IOPs) were excised and analyzed with standard voltage clamp protocols (*5*). Ionic conditions were symmetrical, with the exception of buffered calcium, and contained 140 mM KCl, 0.5 mM $MgCl_2$, and 5 mM Hepes (pH = 7.2).
15. "Cytoplasmic" calcium was changed by perfusing IOPs with solutions buffered with 2 mM of EGTA, Br_2 BAPTA, or nitrilotriacetic acid [the free calcium concentration was determined with MaxChelator software (*27*)]. These concentrations were measured with a calcium electrode (Microelectrodes, Bedford, NH) calibrated with standard solutions obtained from World Precision Instruments (Sarasota, FL).
16. Half-activation voltages were determined by fitting normalized conductance (g/g_{max}) (Figs. 1C and 2, B and D) with a Boltzmann function given by ($\%g/g_{max} = 100/[1 + e^{-(V - V_{1/2})qF/RT}]$), where q is the gating charge, F is Faraday's constant, R is the universal gas constant, and T is the absolute temperature.
17. O. B. McManus *et al.*, *Neuron* **14**, 645 (1995); S. I. Dworetzky *et al.*, *J. Neurosci.* **16**, 4543 (1996); J. Tseng-Crank *et al.*, *Proc. Natl. Acad. Sci. U.S.A.* **93**, 9200 (1996); P. Meera, M. Wallner, Z. Jiang, L. Toro, *FEBS Lett.* **382**, 84 (1996).
18. C. Oberst *et al.*, *Oncogene* **14**, 1109 (1997).
19. Ratios of α cDNA to β cDNA were varied from 1:1 to 1:10 with no differences seen, implying that the effect of β was saturated at the lowest ratio. In most experiments a ratio of 1:2 was used.
20. In these experiments, activation rates were slightly faster upon β combination. This observation is consistent with the hypothesis that β subunits principally affect channel open states, with lesser influence on closed-to-open transitions. Activation steps were made from negative voltages at which the channels were fully closed. Symmetrical slowing of activation and deactivation by β would be expected for small excursions about a voltage level at which some fraction of channels are in the open state, as observed in hair cells (*4*).
21. K_D and δ were determined from the dependence of $V_{1/2}$ on $[Ca^{2+}]$ (Fig. 1D), where $V_{1/2} = -(2.303RT/2\delta F)\log[Ca^{2+}] + (2.303RT/2\delta F)\log[K_D]$ (*28*). δ is the electrical distance traveled by calcium into the membrane; it varied between 0.3 and 0.5.
22. RT-PCR was performed on quail cochlear RNA with the use of primers flanking the untranslated regions of *slo*-β. A full-length product (800 bp) was subcloned and sequenced to confirm its identity.
23. Frozen tissue sections of fixed and decalcified quail temporal bone (16 μm thick) were hybridized with digoxigenin-labeled cRNA (*29*) obtained by in vitro transcription of the full-length RT-PCR product of *slo*-β from quail cochlea. Alkaline phosphatase (AP)–conjugated sheep antibody to digoxigenin was used to detect cRNA-mRNA hybrids. The labeling was visualized with the AP substrates 4-nitro blue tetrazolium chloride and 5-bromo-4-chloro-3-indolylphosphate. All reagents were purchased from Boehringer-Mannheim (Indianapolis, IN).
24. The gradient in β expression, as well as the fact that BK channels are fewest in apical hair cells (*2, 6*), implies that the ratio of β to α is highest in apical hair cells and falls toward the high-frequency base. The stoichiometry of αβ combination was not explicitly tested in these experiments (*19*).
25. C. J. Kros, J. P. Rupersberg, A. Rüsch, *Nature* **394**, 281 (1998).
26. P. A. Fuchs and B. H. A. Sokolowski, *Proc. R. Soc. London Ser. B* **241**, 122 (1990).
27. M. Bers, C. W. Patton, R. Nuccitelli, *Methods Cell Biol.* **40**, 3 (1994).
28. J. Cui, D. H. Cox, R. W. Aldrich, *J. Gen. Physiol.* **109**, 647 (1997).
29. H. Hiel *et al.*, *Brain Res.* **738**, 347 (1996).
30. We thank C. Oberst and K. Bister for their gift of quail *slo*-β. This work was supported by grant DC00276 from the National Institute of Deafness and Communication Disorders.

28 July 1998; accepted 19 November 1998

Female × Male Interactions in *Drosophila* Sperm Competition

Andrew G. Clark,* David J. Begun, Timothy Prout

In several organisms, the success of a male's sperm in multiply inseminated females depends on the male's genotype. In *Drosophila*, the female also plays a role in determining which sperm are successful. Pairwise tests among six isogenic lines of *Drosophila melanogaster* were performed to determine whether there is a genotype-specific interaction in the success of sperm. The success of a particular male's sperm was found to depend on the genotype of the female with which he mates, providing evidence for an interaction with profound evolutionary consequences.

Males and females face very different problems in trying to assure that their gametes are used maximally. Males that can co-opt females into using their sperm are at an advantage over other males. Ignoring the complexities of mating behavior, there is an enormous opportunity for variation in the success of different males' sperm in multiply mated females. Genes that give such an advantage to one male's sperm are expected to increase in the population, even if this increase causes a decline in the viability or fertility of the mother or offspring (*1*). Females cannot afford to let males be the sole determinant of which gametes are used, especially if evolution in males results in deleterious consequences for the female (*2–4*).